AIAA JOURNAL
Vol. 30, No. 4, April 1992

Continuum Design Sensitivity of Transient Responses Using Ritz and Mode Acceleration Methods

Semyung Wang* and Kyung K. Choi†
University of Iowa, Iowa City, Iowa 52242

In this paper, a unified continuum-based sizing design sensitivity analysis method is developed for the transient dynamic response of built-up structures. Using the direct differentiation method, the variational equation of the built-up structure is differentiated with respect to the design variable to obtain a variational design sensitivity equation of the transient response. The same finite element analysis model that is used to obtain an approximate solution of the variational equation of the built-up structure is also used to obtain an approximate solution of the variational design sensitivity equation. For large-size built-up structures, the same superposition method is used both to reduce the dimension of the matrix equation of the built-up structure and also to reduce the dimension of the design sensitivity equation. The continuum-based design sensitivity analysis method can be implemented outside established finite element analysis codes using postprocessing data since it does not require derivatives of the stiffness, damping, and mass matrices. Moreover, the method is efficient since it does not require derivatives of basis vectors. Either the Ritz or mode acceleration method is used to further improve accuracy and efficiency of both analysis and sensitivity results. An example with damping shows that accurate design sensitivity of pointwise transient displacements is obtained using only 10% of basis vectors. This example indicates that in the continuum-based design sensitivity analysis method the same basis vectors that are used for analysis of the built-up structure are suitable for analysis of the design sensitivity equation.

I. Introduction

SINCE a number of design iterations are required in design optimization of large-scale built-up structures, development of an efficient method is especially desirable for transient dynamic analysis and optimization. To achieve this goal, a large amount of research has been carried out in the areas of structural dynamic analysis and design sensitivity analysis during the last 20 years. In structural dynamic analysis, substantial improvements have been made for efficiently obtaining transient dynamic response using the mode acceleration method (MAM),[1,2] the load dependent Ritz vector (LDRV) method,[3-6] and the Lanczos algorithm.[7-9] The MAM is a variation of the mode displacement method (MDM) in which a truncated set of eigenvectors is used as a basis to compensate for the effect of neglected high-frequency modes. For the LDRV method, proposed by Wilson et al.,[3] a sequence of orthogonal Ritz vectors is used. The LDRVs are generated from the externally applied load and are orthonormalized using the Gram-Schmidt orthogonalization procedure. Thus LDRVs can be generated at a fraction of the cost that is required to calculate eigenvectors. The LDRV method has the same effect as MAM since its initial vector is static deflection of the structure. Kline[4] extended the use of LDRVs to the construction of a basis by combining these vectors with eigenvectors. When some eigenvectors are already available, it is easy to increase the accuracy of analysis results by adding a few LDRVs to the basis. Kline claimed that, based on residual errors, the best possible basis may be a combination of eigenvectors and LDRVs. Leger et al.[5] proposed a modified version of the LDRV method, called the Leger-Wilson-Yuan-Dickens (LWYD) algorithm, which eliminates loss of orthogonality, as in the Lanczos method. The Lanczos vectors are identical to LDRVs with the same initial vector but the Lanczos algorithm originates from mathematics, whereas the LDRV method arises from engineering.

In structural design sensitivity analysis (DSA) of the static response and eigenvalue, very good accuracy and efficiency have been achieved using a continuum DSA method. A numerical method has been developed to evaluate continuum DSA results outside established finite element analysis (FEA) codes using postprocessing data only.[10-14] Derivatives of stiffness and mass matrices are not required in the continuum DSA method. However, structural DSA of transient dynamic response has not been well developed yet.

In this paper, a unified continuum-based sizing DSA method is proposed for the transient dynamic response of built-up structures using the direct differentiation method. The proposed method utilizes LDRVs, the MAM, the superposition method, and a parallel computing environment. It should be noted that use of the superposition method is necessary to obtain transient dynamic response of large-scale built-up structures efficiently.

In the continuum-based DSA method, the continuum model of the built-up structure is differentiated with respect to design variable u to obtain a variational equation of design sensitivity z' of the transient response z. Just as the transient response z of the large-scale built-up structure is approximated using the superposition method, design sensitivity z' is represented using a linear combination of the same basis vectors. The reduced governing equation for z' is then solved using the direct integration method.

There are several very attractive features in the proposed continuum-based DSA method. First, as in the static response and eigenvalue cases, the continuum-based DSA method can

Presented as Paper 90-1137 at the 31st AIAA/ASME/ASCE/AHS/ASC Structures, Structural Dynamics, and Materials Conference, Long Beach, CA, April 2–4, 1990; received Nov. 28, 1990, revision received May 14, 1991; accepted for publication May 17, 1991.

*Postdoctoral Associate, Department of Mechanical Engineering, Center for Simulation and Design Optimization. Student Member AIAA.

†Professor and Associate Director, Department of Mechanical Engineering, Center for Simulation and Design Optimization. Member AIAA.

be implemented outside established FEA codes using postprocessing data since it does not require derivatives of stiffness, damping, and mass matrices.[10–14] Second, the method is efficient because design sensitivity z' can be obtained without computing derivatives of basis vectors. Third, the method is efficient since LDRVs, instead of eigenvectors, are used to form a basis.[3,4] Moreover, as mentioned before, the use of LDRVs improves the accuracy of analysis results.[3–6] Fourth, if necessary, more LDRVs can be added to the basis to represent design sensitivity z', thereby improving the accuracy of design sensitivity results without significantly increasing the computation time. Also, a smaller time step can be used for analysis of the sensitivity equation of z' if necessary. If the MAM was used for the original analysis, it can be used to obtain design sensitivity. Last, the direct differentiation method is more attractive for DSA of transient dynamic response since it is not necessary to store the transient response of the built-up structure during forward integration and to use it during backward integration as in the adjoint variable method.[15] The continuum-based DSA method is well suited for built-up structures with nonproportional damping since the combination of mode superposition and direct integration methods is known to be the most efficient method for these types of structures. The dimension of the system equation is reduced by the superposition method, and errors due to coupling are eliminated by the direct integration method.

II. Variational Equation for Structural Dynamics

The equation of dynamics for a built-up structure can be written in the form[10]

$$m(x,u)z_{tt} + c(x,u)z_t + A_u z = f(x,t,u), \quad x \in \Omega, \quad t \geq 0 \tag{1}$$

with initial conditions

$$z(x,0,u) = z^0(x,u), \quad z_t(x,0,u) = z_t^0(x,u), \quad x \in \Omega \tag{2}$$

where Ω is the domain of the structure; t the time, u the design variable; $z(x,t,u)$ the transient response; $m(x,u)$ and $c(x,u)$, which represent mass and damping effects in the structure, respectively, are taken to be design dependent; and $f(x,t,u)$ is the applied dynamic load. The operator A_u is a spatial partial differential operator, and the design variable $u(x)$ is independent of time. Also, $z(x,t,u)$ must satisfy homogeneous boundary conditions specified for the built-up structure.

A variational form of Eq. (1) can be obtained by multiplying both sides by an arbitrary virtual displacement $\bar{z}(x)$ and integrating over the physical domain

$$\int\int_\Omega \bar{z}[m(x,u)z_{tt} + c(x,u)z_t + A_u z]\, d\Omega = \int\int_\Omega \bar{z}f(x,t,u)\, d\Omega, \quad t \geq 0 \tag{3}$$

Using the energy bilinear forms, load linear form, and boundary conditions of the built-up structure, Eq. (3) can be rewritten as

$$d_u(z_{tt},\bar{z}) + \int\int_\Omega \bar{z}c(x,u)z_t\, d\Omega + a_u(z,\bar{z}) = l_u(\bar{z}), \quad t \geq 0 \tag{4}$$

which must hold for all kinematically admissible virtual displacements $\bar{z} \in Z$. In Eq. (4),

$$d_u(z_{tt},\bar{z}) \equiv \int\int_\Omega \bar{z}m(x,u)z_{tt}\, d\Omega \tag{5}$$

$$a_u(z,\bar{z}) \equiv \int\int_\Omega \bar{z}A_u z\, d\Omega \tag{6}$$

$$l_u(\bar{z}) \equiv \int\int_\Omega \bar{z}f(x,t,u)\, d\Omega \tag{7}$$

are the kinetic and strain energy bilinear forms and the load linear form, respectively.

III. Approximate Dynamic Analysis

Since analytical solutions of Eq. (4) cannot be obtained for complex structures, an FEA method is usually used for an approximate solution. Using the FEA method, the approximate matrix equation of Eq. (4) is

$$M\ddot{z}(t) + C\dot{z}(t) + Kz(t) = F(t) \tag{8}$$

for $t \geq 0$, where M, C, and K are $n \times n$ mass, damping, and stiffness matrices, respectively, and $F(t)$ is the external load vector. Initial conditions $z(0)$ and $\dot{z}(0)$ can be obtained by evaluating the initial conditions of Eq. (2) at nodal points. The notation $z(t)$ is used in Eq. (8) even though the $n \times 1$ vector $z(t)$ is a discretization of the transient response $z(x,t,u)$ of Eq. (4).

For practical computation for large built-up structures, depending on the basis used, the transient response is approximated by a linear combination of eigenvectors and/or Ritz vectors using the MDM, MAM, and LDRV methods. In approximating the transient response, $z(t)$ is

$$z(t) = \sum_{i=1}^{m} v_i(t)\phi^i = \Phi v(t) \tag{9}$$

where $m < n$, $\Phi = [\phi^1,\phi^2,\ldots,\phi^m]$, and $v(t) \in R^m$. In Eq. (9), ϕ^i can be the eigenvector y^i or the Ritz vector r^i such that

$$Ky^i = \zeta_i My^i \tag{10}$$

$$y^{iT}My^i = r^{iT}Mr^i = \phi^{iT}M\phi^i = \delta_{ij} \tag{11}$$

where δ_{ij} is the Kronecker delta. Thus, $\Phi^T M\Phi = I$. Substituting Eq. (9) into Eq. (8) and premultiplying the resulting matrix equation by Φ^T,

$$\ddot{v}(t) + \Phi^T C\Phi\dot{v}(t) + \Phi^T K\Phi v(t) = \Phi^T F(t) \tag{12}$$

for $t \geq 0$, with initial conditions

$$v(0) = \Phi^T Mz(0), \quad \dot{v}(0) = \Phi^T M\dot{z}(0) \tag{13}$$

which can be obtained from Eq. (9). Note that Eq. (12) is an ordinary differential equation. Once the solution $v(t)$ of Eq. (12) is obtained, the approximate transient response $z(t)$ can be obtained from Eq. (9). If all of the ϕ^i are eigenvectors, then the MDM or MAM is applicable. On the other hand, if all ϕ^i are Ritz vectors, then the LDRV method is applicable. For the Kline method, ϕ^i is a combination of eigenvectors y^i and Ritz vectors r^i.

IV. Continuum Design Sensitivity Analysis

For DSA of the transient dynamic response of structural systems, two methods are generally used: the direct differentiation and adjoint variable methods.[15–18] The latter method has been more commonly used because it can handle a large number of design variables; however, it suffers from a few drawbacks when used for the transient dynamic response of built-up structures. First, during forward integration of the state equations, information must be saved to be retrieved at an appropriate time step during the backward integration of the adjoint equations. Another drawback of the method is the difficulty of positive error control during numerical integration of the state and adjoint equations. Since backward integration can be started after forward integration is completed, it is hard to estimate how the error in the forward integration will influence the solution during the following backward integration.

With the development of parallel computing techniques, the

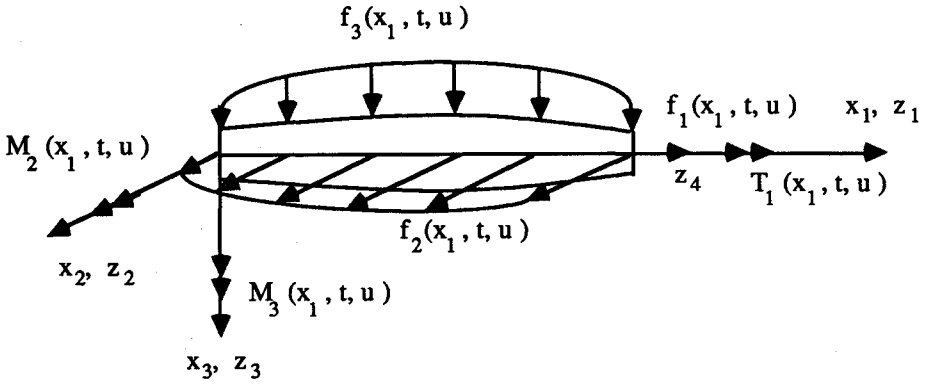

Fig. 1 Truss/beam structural component.

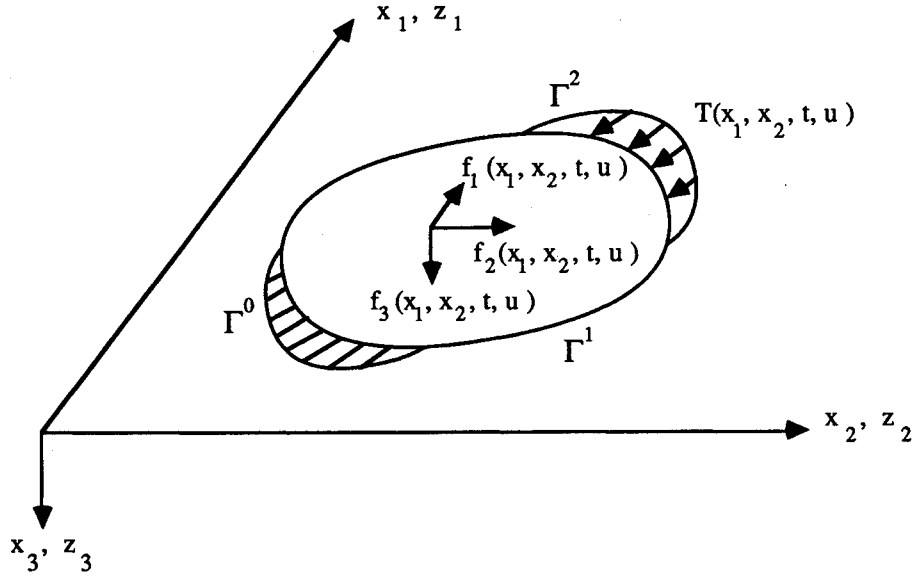

Fig. 2 Plane elastic solid/plate structural component.

direct differentiation method has become attractive since each set of sensitivity equations corresponding to a design variable is independent and can be assigned to a processor in a parallel computer. The adjoint variable method, on the other hand, is not suitable for parallel computing because of the sequential computation procedure and data dependency during the forward and backward integration.

In this section, a continuum-based DSA method for transient dynamic response that does not require design sensitivity of basis vectors is proposed. In this method, approximation is not involved until a variational equation for z' is obtained. This approach is computationally attractive since derivatives of the basis vectors are not required. The proposed method is applicable for any analysis method, such as the MDM, MAM, and LDRV methods, since only the basis vectors and the corresponding responses are required in this design sensitivity formulation.

Take the design variation of Eq. (4) to obtain

$$d'_{\delta u}(z_{tt},\bar{z}) + d_u(z'_{tt},\bar{z}) + \iint_\Omega [\bar{z}c_{,u}z_t\delta u + \bar{z}cz'_t]\,d\Omega + a'_{\delta u}(z,\bar{z}) + a_u(z',\bar{z}) = l'_{\delta u}(\bar{z}), \quad t \geq 0 \tag{14}$$

for all $\bar{z} \in Z$ where the subscript u in $c_{,u}$ denotes partial differentiation with respect to the design variable u. In Eq. (14),

$$z' = z'(x,t,u) \equiv \frac{d}{d\tau} z(x,t,u + \tau\delta u)|_{\tau=0} \tag{15}$$

is the first variation of z with respect to the design variable u in the direction δu of the design change. Also, from Eq. (2),

$$z'(x,0,u) = z^{0'}(x,u), \quad z'_t(x,0,u) = z_t^{0'}(x,u) \tag{16}$$

where $z'(x,t,u)$ satisfies the same homogeneous boundary conditions as $z(x,t,u)$. Rearranging Eq. (14),

$$d_u(z'_{tt},\bar{z}) + \iint_\Omega \bar{z}cz'_t\,d\Omega + a_u(z',\bar{z}) = -d'_{\delta u}(z_{tt},\bar{z}) - \iint_\Omega \bar{z}c_{,u}z_t\delta u\,d\Omega - a'_{\delta u}(z,\bar{z}) + l'_{\delta u}(\bar{z}), \quad t \geq 0 \tag{17}$$

for all $\bar{z} \in Z$. Equation (17) is a variational equation with design sensitivity $z'(x,t,u)$ as the unknown. That is, if the solution $z(x,t,u)$ of Eq. (4) is obtained, the right side of Eq. (17) can be computed to obtain the fictitious load.

Just as with the continuum equation (4), since the analytical solution of Eq. (17) cannot be obtained for complex structures, the FEA method is used for an approximate solution. Using the FEA method, the approximate matrix equation of Eq. (17) is

$$M\ddot{z}'(t) + C\dot{z}'(t) + Kz'(t) = F_f(t) \tag{18}$$

with initial conditions $z'(0)$ and $\dot{z}'(0)$ that can be obtained by evaluating the initial conditions of Eq. (16) at nodal points.

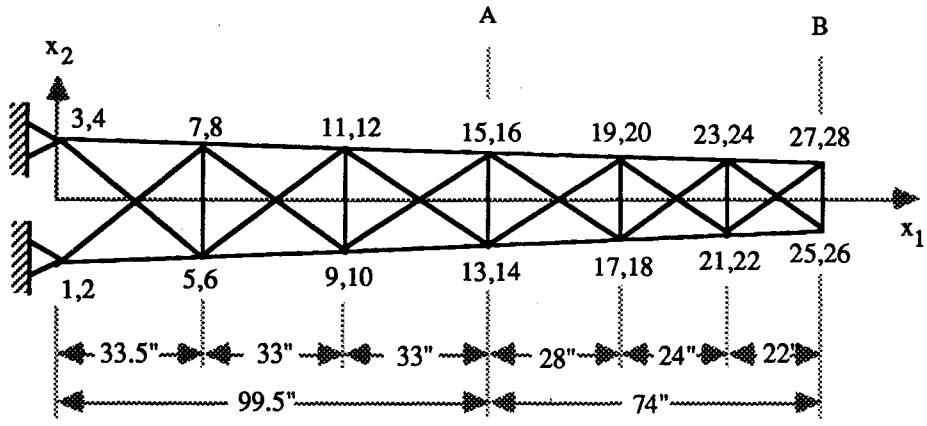

a) Top view

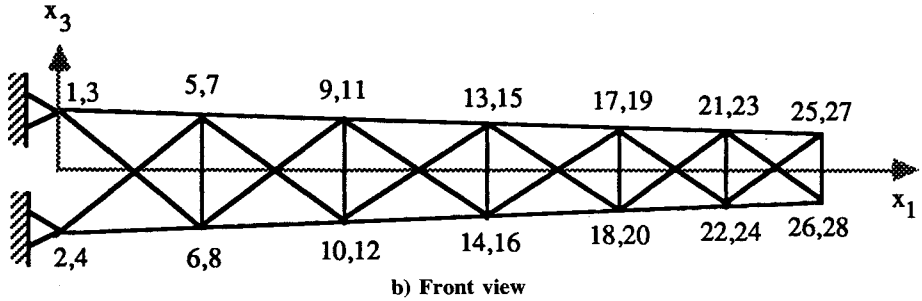

b) Front view

Fig. 3 Helicopter tail boom truss.

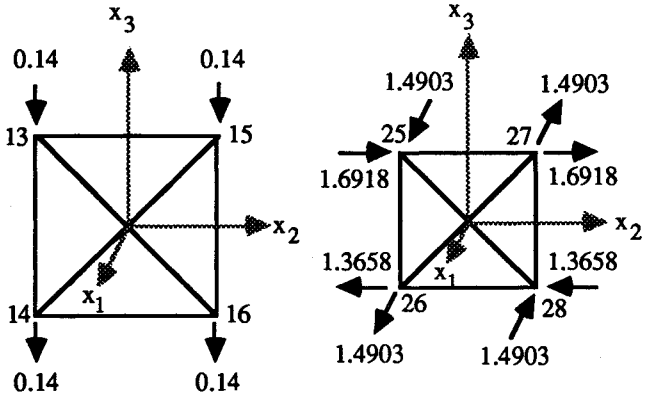

a) Loads at section A b) Loads at section B

Fig. 4 Load data for tail boom truss.

For efficient computation of $z'(t)$, the same superposition method used in Sec. III is used; i.e., let $z'(t)$ be approximated by

$$z'(t) = \sum_{i=1}^{k} w_i(t)\phi^i = \Phi w(t), \quad m \leq k < n \tag{19}$$

where m is the number of basis vectors used for the original analysis, and k is the number of basis vectors used for the sensitivity analysis. In Eq. (19), ϕ^i is either eigenvector y^i or the Ritz vector r^i that satisfies Eqs. (10) and (11), $\Phi = [\phi^1,\phi^2,\ldots,\phi^k]$, $w(t) \in R^k$, and $\Phi^T M \Phi = I$.

Substituting Eq. (19) into Eq. (18) and premultiplying the resulting matrix equation by Φ^T,

$$\ddot{w}(t) + \Phi^T C \Phi \dot{w}(t) + \Phi^T K \Phi w(t) = \Phi^T F_f(t) \tag{20}$$

for $t \geq 0$, with initial conditions

$$w(0) = \Phi^T M z'(0), \quad \dot{w}(0) = \Phi^T M \dot{z}'(0) \tag{21}$$

Note that dimension k of the sensitivity equation (20) is not necessarily the same as dimension m of the original equation [Eq. (12)]. The coupled equation (20) can be solved by the direct integration method to obtain $w(t)$. To evaluate $F_f(t)$ in Eq. (18), $d'_{\delta u}(z_{tt},\bar{z})$, $c_{,u}$, $a'_{\delta u}(z,\bar{z})$, and $l'_{\delta u}(\bar{z})$ in Eq. (17) must be computed for perturbation of each design parameter. Once $w(t)$ is obtained, the approximate design sensitivity $z'(t)$ can be obtained from Eq. (19).

If the MAM was used for the original analysis, Eq. (19) is modified to

$$z'(t) = \Phi w(t) + K^{-1} F_f(t) - \Phi \Lambda^{-1} \Phi^T F_f(t) \tag{22}$$

where the basis vectors are all eigenvectors. For proportional damping, $w(t)$ can be obtained from the uncoupled equation

$$\ddot{w}_i + 2\zeta_i \omega_i \dot{w}_i + \omega_i^2 w_i = \phi^{iT} F_f(t) \tag{23}$$

instead of the coupled equation (20). For Rayleigh damping, $2\zeta_i\omega_i$ in Eq. (23) is replaced with $\alpha + \beta\omega_i^2$, where α and β are damping coefficients that define the damping matrix, $C = \alpha M + \beta K$.

For design optimization of built-up structures with transient dynamic response, treatment of the pointwise constraint is important. A general pointwise constraint on transient response that must hold for all time and at every point of domain Ω can be defined as

$$g[z(x,t,u),u] \leq 0, \quad x \in \Omega, t \in [0,T] \tag{24}$$

The pointwise constraint of Eq. (24) can be approximated using an equivalent functional constraint of the form,[19]

$$\int_0^T \int\int_\Omega \{g[z(x,t,u),u]\}^+ \, d\Omega \, dt \leq 0 \tag{25}$$

where

$$\{g[z(x,t,u),u]\}^+ = \max_{\substack{x\in\Omega \\ t\in[0,T]}} \{0, g[z(x,t,u),u]\} \tag{26}$$

Use of the functional of Eq. (25) provides the capability for reducing constraint errors in Eq. (24) to near zero for some problems.[19] However, as the error approaches zero, the time and physical domains over which the integrand is defined reduces to infinitesimal size and, thus, a singular functional occurs. Also, it introduces an implicit assumption in the necessary optimality conditions; i.e., the Lagrange multiplier function for the constraint is either constant or zero throughout the time and physical domains.

The second method of approximating Eq. (24) can be obtained using a worst-case design technique

$$g[z(x_i,t_i,u),u] \le 0, \quad i = 1 \sim p \tag{27}$$

Table 1 Design data for tail boom truss (modulus of elasticity = 1.05D+07 psi; material density = 0.10 lb/in.^{3})

Design variables		
Design variable No.	Member No.	Value (in.^{2})
1	2,3	1.3750
2	1,4	1.3710
3	5,6,9,10	0.1375
4	7,8,11,12	0.1395
5	13,15	0.0415
6	14,16	0.0821
7	17,18	0.0415
8	20,21	1.2420
9	19,22	1.2390
10	23,24,27,28	0.1741
11	25,26,29,30	0.1649
12	31,33	0.0415
13	32,34	0.1002
14	35,36	0.0415
15	38,39	1.0290
16	37,40	1.0280
17	41,42,45,46	0.2110
18	43,44,47,48	0.2295
19	49,51	0.0415
20	50,52	0.1371
21	53,54	0.0415
22	56,57	0.8221
23	55,58	0.8226
24	59,60,63,64	0.2365
25	61,62,65,66	0.2587
26	67,69	0.0415
27	68,70	0.1575
28	71,72	0.0415
29	74,75	0.5806
30	73,76	0.5830
31	77,78,81,82	0.2675
32	79,80,83,84	0.2883
33	85,87	0.0415
34	86,88	0.1934
35	89,90	0.0415
36	92,93	0.2299
37	91,94	0.2090
38	95,96,99,100	0.3295
39	97,98,101,102	0.3428
40	103,105	0.0564
41	104,106	0.1036
42	107,108	0.1987

where (x_i,t_i) are the local maximum points and p is the number of local maximum points for the constraint g. This formulation does not assume the Lagrange multiplier to be constant over the time and physical domains. However, this method requires a large amount of computational effort to locate the precise local maximum points on the time and physical domains. Moreover, the pointwise constraint may not be differentiable at the local maximum points.

The third method of approximating the pointwise constraint of Eq. (24) can be developed using an averaging multiplier technique,[10]

$$\int_0^T \int\int_\Omega m(x,t,\bar{x},\bar{t}) g[z(x,t,u),u]\, d\Omega\, dt \le 0 \tag{28}$$

where the characteristic function $m(x,t,\bar{x},\bar{t})$ is defined to be zero everywhere except on a subdomain that contains the point $(\bar{x},\bar{t})$. On the subdomain, the characteristic function m has a constant value and satisfies the condition

$$\int_0^T \int\int_\Omega m(x,t,\bar{x},\bar{t})\, d\Omega\, dt = 1 \tag{29}$$

The characteristic function m approaches the Dirac distribution as the subdomain shrinks to the point $(\bar{x},\bar{t})$. Although some error is involved in Eq. (28), quite good numerical results can be obtained using the characteristic function m that is defined on a finite subdomain.[10]

The approximation methods given in Eqs. (25) and (28) are written in integral form. Thus, a general performance measure can be written as

$$\Psi = \int_0^T \int\int_\Omega g(z,\nabla z,u)\, d\Omega\, dt \tag{30}$$

where the transient response z of the built-up structure is design dependent; i.e., $z = z(x,t,u)$. Taking a first-order design variation of Eq. (30),

$$\Psi' = \int_0^T \int\int_\Omega [g_z z' + g_{\nabla z} \nabla z' + g_u \delta u]\, d\Omega\, dt \tag{31}$$

For the direct differentiation method, $z'(t)$ is obtained from Eqs. (19) and (20) for the LDRV method or from Eqs. 20 [or (23)] and (22) for the MAM. For the displacement at any point in an element, the design sensitivity can be obtained by interpolating $z'(t)$ at nodal points using the shape function. Once $z'(x,t)$ is obtained, Eq. (31) can be evaluated numerically to obtain the design sensitivity.

V. Structural Components

In this section, the energy bilinear and load linear forms of the truss/beam and plane elastic solid/plate design components are provided. The first variations of these forms that can be used to evaluate $F_f(t)$ in Eq. (18) are derived.

A. Truss/Beam Design Component

The kinetic and strain energy bilinear forms of the truss/beam structural component, shown in Fig. 1, are

Table 2 Sizing design sensitivity of transient displacements with respect to the first design variable for tail boom using 10 eigenvectors and 5 Ritz vectors at 0.016 s (α = 0.1318D+02, β = 0.2132D−04, 2% perturbation)

Node	DOF	$\Psi(u)$	$\Delta\Psi$	Ψ'	$\Delta\Psi/\Psi'$, %	$\Delta\Psi_E/\Psi'$, %	$\Delta\Psi_E/\Delta\Psi$, %	Ψ_E/Ψ, %	Ψ_E/Ψ, %	Ψ_E/Ψ, %
25	x_2	0.7429D+0	−0.1998D−2	−0.2030D−2	98.4	102.6	104.2	100.0	200.2	88.7
26	x_2	0.5787D+0	−0.2477D−2	−0.2460D−2	100.7	100.4	100.0	100.1	103.5	121.5
27	x_2	0.7430D+0	−0.1997D−2	−0.2029D−2	98.5	102.5	104.1	100.0	201.3	89.1
28	x_2	0.5787D+0	−0.2477D−2	−0.2460D−2	100.7	100.5	99.8	100.1	103.6	121.1

Table 3 Sizing design sensitivity of transient displacements with respect to the first design variable for tail boom using 10 eigenvectors and 5 Ritz vectors at 0.047 s (α = 0.1318D+02, β = 0.2132D−04, 2% perturbation)

Node	DOF	$\Psi(u)$	$\Delta\Psi$	Ψ'	$\Delta\Psi/\Psi'$ %	$\Delta\Psi_E/\Psi'$, %	$\Delta\Psi_E/\Delta\Psi$, %	Ψ_E/Ψ, %	$\dot{\Psi}_E/\dot{\Psi}$, %	$\ddot{\Psi}_E/\ddot{\Psi}$, %
25	x_2	0.7033D+0	−0.3796D−2	−0.3803D−2	99.8	98.0	98.2	99.8	82.0	78.1
26	x_2	0.4305D+0	−0.3052D−2	−0.3057D−2	99.8	99.8	99.9	100.3	99.2	98.9
27	x_2	0.7032D+0	−0.3795D−2	−0.3801D−2	99.8	98.0	98.2	99.8	82.1	78.1
28	x_2	0.4306D+0	−0.3052D−2	−0.3057D−2	99.8	99.7	99.9	100.3	99.1	98.9

Table 4 Sizing design sensitivity of transient displacements with respect to the first design variable for tail boom using 15 eigenvectors at 0.016 s (α = 0.1318D+02, β = 0.2132D−04, 2% perturbation)

Node	DOF	$\Psi(u)$	$\Delta\Psi$	Ψ'	$\Delta\Psi/\Psi'$, %	$\Delta\Psi_E/\Psi'$, %	$\Delta\Psi_E/\Delta\Psi$, %	Ψ_E/Ψ, %	$\dot{\Psi}_E/\dot{\Psi}$, %	$\ddot{\Psi}_E/\ddot{\Psi}$, %
25	x_2	0.7410D+0	−0.20863D−2	−0.2062D−2	101.2	101.0	99.8	99.7	123.1	61.3
26	x_2	0.5775D+0	−0.2466D−2	−0.2483D−2	99.3	99.4	100.1	99.9	91.8	97.4
27	x_2	0.7410D+0	−0.2085D−2	−0.2060D−2	101.2	101.0	99.8	99.7	124.3	61.4
28	x_2	0.5775D+0	−0.2466D−2	−0.2484D−2	99.3	99.5	100.2	99.9	91.1	97.2

Table 5 Sizing design sensitivity of transient displacements with respect to the first design variable for tail boom using 15 eigenvectors at 0.047 s (α = 0.1318D+02, β = 0.2132D−04, 2% perturbation)

Node	DOF	$\Psi(u)$	$\Delta\Psi$	Ψ'	$\Delta\Psi/\Psi'$, %	$\Delta\Psi_E/\Psi'$, %	$\Delta\Psi_E/\Delta\Psi$, %	Ψ_E/Ψ, %	$\dot{\Psi}_E/\dot{\Psi}$, %	$\ddot{\Psi}_E/\ddot{\Psi}$, %
25	x_2	0.7047D+0	−0.3783D−2	−0.3773D−2	100.3	98.8	98.5	100.0	86.4	98.6
26	x_2	0.4303D+0	−0.3058D−2	−0.3057D−2	100.1	99.8	99.7	100.2	99.2	108.3
27	x_2	0.7047D+0	−0.3783D−2	−0.3773D−2	100.3	98.8	98.5	100.0	86.4	98.6
28	x_2	0.4304D+0	−0.3058D−2	−0.3057D−2	100.0	99.8	99.7	100.2	99.2	108.3

Table 6 Sizing design sensitivity of transient displacements with respect to the first design variable for tail boom using six eigenvectors and three Ritz vectors at 0.016 s (α = 0.1318D+02, β = 0.2132D−04, 2% perturbation)

Node	DOF	$\Psi(u)$	$\Delta\Psi$	Ψ'	$\Delta\Psi/\Psi'$, %	$\Delta\Psi_E/\Psi'$, %	$\Delta\Psi_E/\Delta\Psi$, %	Ψ_E/Ψ, %	$\dot{\Psi}_E/\dot{\Psi}$, %	$\ddot{\Psi}_E/\ddot{\Psi}$, %
25	x_2	0.7268D+0	−0.2108D−2	−0.2114D−2	99.8	98.5	98.8	97.8	76.4	−59.5
26	x_2	0.5855D+0	−0.2303D−2	−0.2320D−2	99.2	106.4	107.2	101.3	264.0	189.8
27	x_2	0.7269D+0	−0.2108D−2	−0.2113D−2	99.8	98.4	98.7	97.8	76.7	−59.1
28	x_2	0.5855D+0	−0.2303D−2	−0.2321D−2	99.2	106.5	107.3	101.3	261.4	189.2

Table 7 Sizing design sensitivity of transient displacements with respect to the first design variable for tail boom using six eigenvectors and three Ritz vectors at 0.047 s (α = 0.1318D+02, β = 0.2132D−04, 2% perturbation)

Node	DOF	$\Psi(u)$	$\Delta\Psi$	Ψ'	$\Delta\Psi/\Psi'$, %	$\Delta\Psi_E/\Psi'$, %	$\Delta\Psi_E/\Delta\Psi$, %	Ψ_E/Ψ, %	$\dot{\Psi}_E/\dot{\Psi}$, %	$\ddot{\Psi}_E/\ddot{\Psi}$, %
25	x_2	0.7023D+0	−0.3538D−2	−0.3577D−2	98.9	104.2	105.3	99.6	138.6	72.8
26	x_2	0.4314D+0	−0.3089D−2	−0.3018D−2	102.3	101.0	98.7	100.5	98.6	115.4
27	x_2	0.7024D+0	−0.3536D−2	−0.3575D−2	98.9	104.2	105.4	99.7	138.5	73.1
28	x_2	0.4314D+0	−0.3091D−2	−0.3020D−2	102.3	101.0	98.7	100.5	98.6	115.1

Table 8 Sizing design sensitivity of transient displacements with respect to the first design variable for tail boom using seven eigenvectors at 0.016 s (α = 0.1318D+02, β = 0.2132D−04, 2% perturbation)

Node	DOF	$\Psi(u)$	$\Delta\Psi$	Ψ'	$\Delta\Psi/\Psi'$, %	$\Delta\Psi_E/\Psi'$, %	$\Delta\Psi_E/\Delta\Psi$, %	Ψ_E/Ψ, %	$\dot{\Psi}_E/\dot{\Psi}$, %	$\ddot{\Psi}_E/\ddot{\Psi}$, %
25	x_2	0.7361D+0	−0.20733D−2	−0.2077D−2	99.8	100.2	100.4	99.1	132.6	26.2
26	x_2	0.5811D+0	−0.2339D−2	−0.2342D−2	99.9	105.4	105.6	100.5	246.7	133.9
27	x_2	0.7361D+0	−0.2072D−2	−0.2076D−2	99.8	100.2	100.4	99.1	134.6	26.3
28	x_2	0.5811D+0	−0.2340D−2	−0.2343D−2	99.9	105.5	105.6	100.5	243.6	133.8

Table 9 Sizing design sensitivity of transient displacements with respect to the first design variable for tail boom using seven eigenvectors at 0.047 s (α = 0.1318D+02, β = 0.2132D−04, 2% perturbation)

Node	DOF	$\Psi(u)$	$\Delta\Psi$	Ψ'	$\Delta\Psi/\Psi'$, %	$\Delta\Psi_E/\Psi'$, %	$\Delta\Psi_E/\Delta\Psi$, %	Ψ_E/Ψ, %	$\dot{\Psi}_E/\dot{\Psi}$, %	$\ddot{\Psi}_E/\ddot{\Psi}$, %
25	x_2	0.7027D+0	−0.3787D−2	−0.3787D−2	100.0	98.4	98.4	99.7	85.4	73.9
26	x_2	0.4317D+0	−0.3077D−2	−0.3058D−2	100.6	99.7	99.1	100.4	98.7	117.7
27	x_2	0.7027D+0	−0.3785D−2	−0.3786D−2	100.0	98.4	98.5	99.7	85.4	74.0
28	x_2	0.4312D+0	−0.3078D−2	−0.3059D−2	100.6	99.7	99.1	100.4	98.7	117.5

$$d_u(z_{tt},\bar{z}) = \int_0^L \rho\left(h\sum_{i=1}^{3} z_{i,tt}\bar{z}_i + Jz_{4,tt}\bar{z}_4\right) dx_1 \quad (32)$$

$$a_u(z,\bar{z}) = \int_0^L (Ehz_{1,1}\bar{z}_{1,1} + EI_3z_{2,11}\bar{z}_{2,11} + EI_2z_{3,11}\bar{z}_{3,11} + GJz_{4,1}\bar{z}_{4,1})\, dx_1 \quad (33)$$

where z_1, z_2, and z_3 are the axial displacement and two orthogonal lateral displacements, respectively; z_4 is the angle of twist; and $z = [z_1,z_2,z_3]^T$. In Eqs. (32) and (33), ρ is the mass density, E the Young's modulus, G the shear modulus, and h, I_2, I_3, and J are the cross-sectional area, two moments of inertia, and the torsional moment of inertia, respectively. Also, the dissipative energy due to Rayleigh damping is

$$\int_0^L \bar{z}c_u z_t\, dx_1 = \alpha d_u(z_t,\bar{z}) + \beta a_u(z_t,\bar{z}) \quad (34)$$

where α and β are damping coefficients. Note that bending and torsional terms are excluded from the energy bilinear forms when only the truss component is considered.

The load linear form of the external loads shown in Fig. 1 is

$$l_u(\bar{z}) = \int_0^L \left(\sum_{i=1}^{3} f_i\bar{z}_i + T_1\bar{z}_4 + M_2\bar{z}_{3,1} + M_3\bar{z}_{2,1}\right) dx_1 \quad (35)$$

where f_1, f_2, and f_3 are the axial and two orthogonal lateral loads, respectively. Also, T_1 is the torque, and M_2 and M_3 are two moments. If only the truss component is considered, torsional load and bending moment are excluded.

The first variations of the energy bilinear and load linear forms of Eqs. (32–35) can be taken as

$$d'_{\delta u}(z_{tt},\bar{z}) = \int_0^L \rho\left(h_{,u}\sum_{i=1}^{3} z_{i,tt}\bar{z}_i + J_{,u}z_{4,tt}\bar{z}_4\right)\delta u\, dx_1 \quad (36)$$

$$a'_{\delta u}(z,\bar{z}) = \int_0^L (Eh_{,u}z_{1,1}\bar{z}_{1,1} + EI_{3,u}z_{2,11}\bar{z}_{2,11} + EI_{2,u}z_{3,11}\bar{z}_{3,11} + GJ_{,u}z_{4,1}\bar{z}_{4,1})\delta u\, dx_1 \quad (37)$$

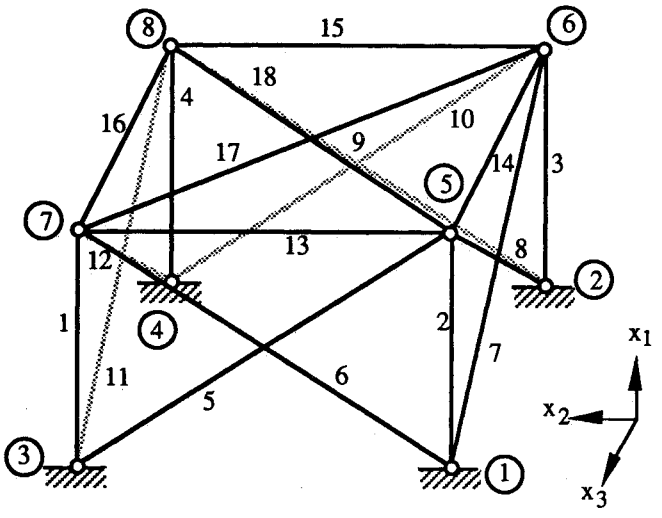

Fig. 5 Member numbering for the first panel.

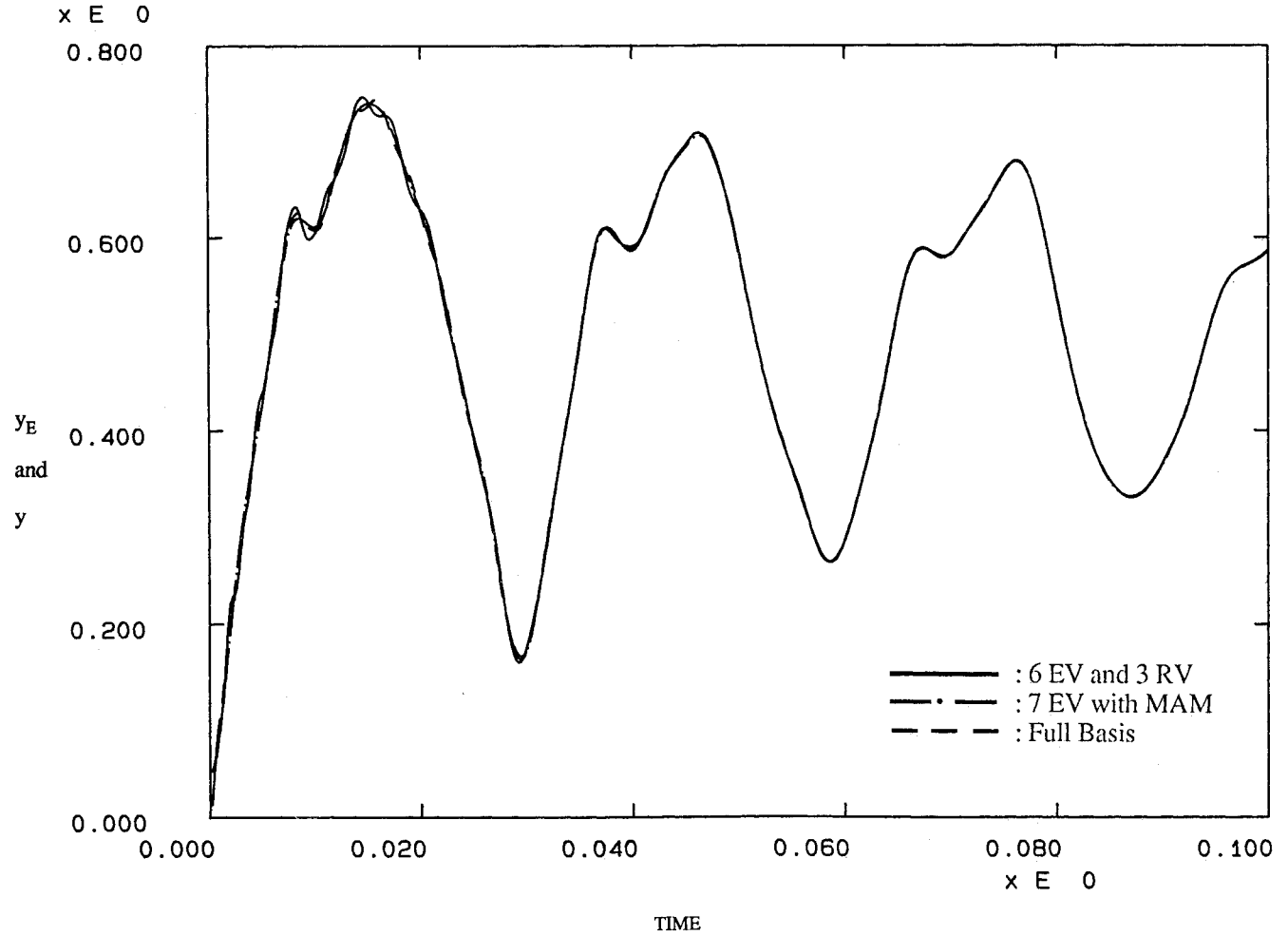

Fig. 6 Comparison of y displacement at node 27 using the LDRV method and MAM.

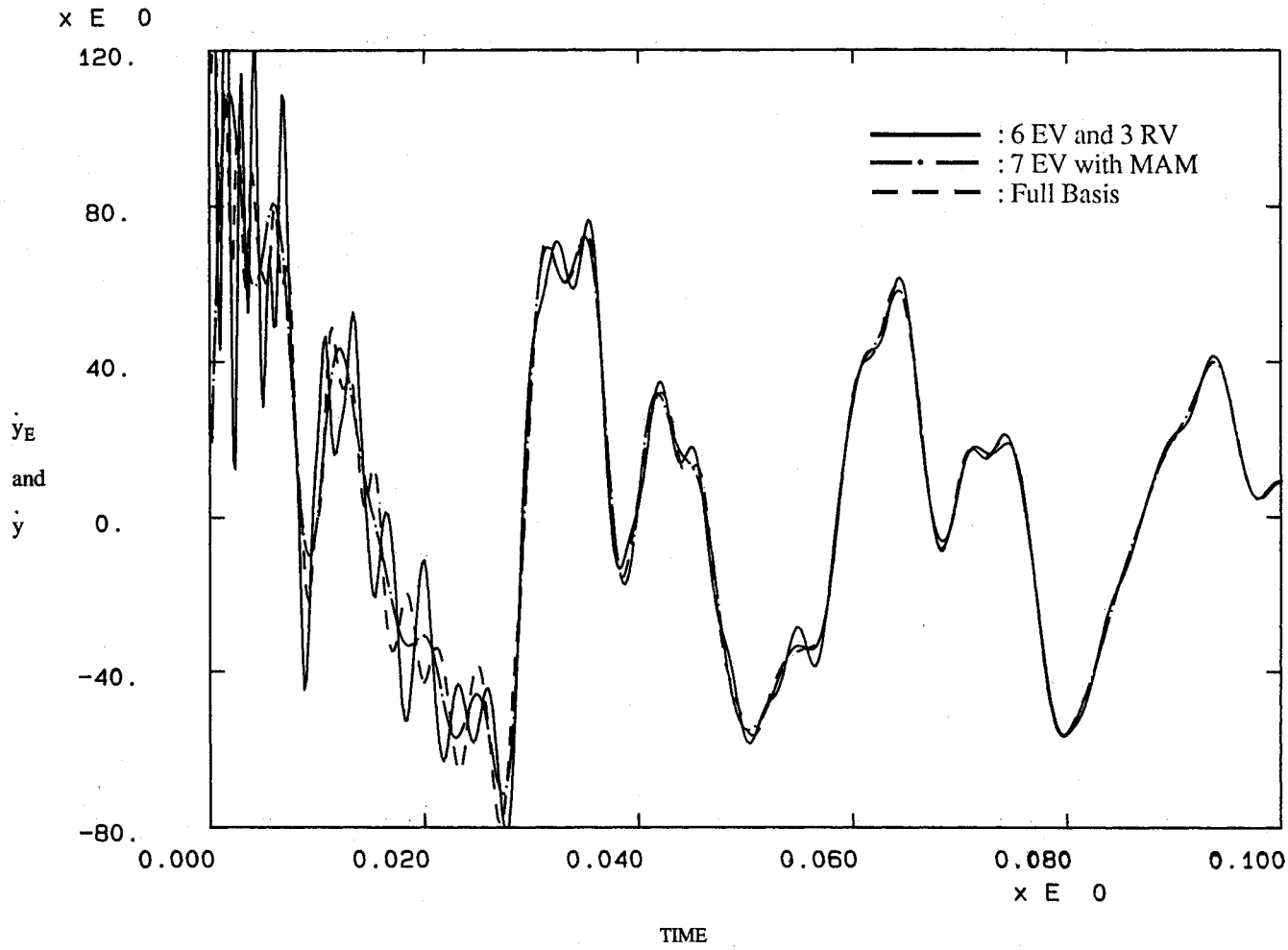

Fig. 7 Comparison of y velocity at node 27 using the LDRV method and MAM.

$$\int_0^L \bar{z}c_{,u}z_t \, dx_1 = \alpha d'_{\delta u}(z_t,\bar{z}) + \beta a'_{\delta u}(z_t,\bar{z}) \tag{38}$$

$$l'_{\delta u}(\bar{z}) = \int_0^L \left(\sum_{i=1}^{3} f_{i,u}\bar{z}_i + T_{1,u}\bar{z}_4 + M_{2,u}\bar{z}_{3,1} + M_{3,u}\bar{z}_{2,1} \right) \delta u \, dx_1 \tag{39}$$

where subscript u denotes the derivatives of terms with respect to design variable u.

Consider a performance measure representing a displacement at a discrete point $\hat{x}_1$ as

$$\Psi_1 = \int_0^T \int_0^L \hat{\delta}(x_1 - \hat{x}_1) z \, dx_1 \, dt \tag{40}$$

where $\hat{\delta}$ is the Dirac delta distribution. The first variation of the performance measure Ψ_1 is

$$\Psi'_1 = \int_0^T \int_0^L \hat{\delta}(x_1 - \hat{x}_1) z' \, dx_1 \, dt \tag{41}$$

B. Plane Elastic Solid/Plate Design Component

Consider the plane elastic solid/plate structural component in Fig. 2. The sizing design variable $u = h(x_1,x_2)$ is the thickness of the structural component. The kinetic and strain energy bilinear forms of the structural component are

$$d_u(z_{tt},\bar{z}) = \int\int_\Omega \rho h \sum_{i=1}^{3} z_{i,tt}\bar{z}_i \, d\Omega \tag{42}$$

$$a_u(z,\bar{z}) = \int\int_\Omega \left[h \sum_{i,j=1}^{2} \sigma^{ij}(v)\epsilon^{ij}(\bar{v}) + \frac{h}{3} \sum_{i,j=1}^{2} \sigma^{ij}(z_3)\epsilon^{ij}(\bar{z}_3) \right] d\Omega \tag{43}$$

where $v = [z_1,z_2]^T$ for the plane elastic solid component. Also, the dissipative energy due to Rayleigh damping is

$$\int\int_\Omega \bar{z}c_u z_t \, d\Omega = \alpha d_u(z_t,\bar{z}) + \beta a_u(z_t,\bar{z}) \tag{44}$$

where α and β are damping coefficients. Note that the bending terms are excluded from the energy bilinear form when only the plane elastic solid structural component is considered.

The load linear form of the external loads shown in Fig. 2 is

$$l_u(\bar{z}) = \int\int_\Omega \sum_{i=1}^{3} f_i\bar{z}_i \, d\Omega + \int_{\Gamma^2} \sum_{i=1}^{2} T_i\bar{z}_i \, d\Gamma \tag{45}$$

where f_1, f_2, and f_3 are two inplane loads and a lateral load, respectively, and $T = [T_1,T_2]^T$ is a traction load. The lateral load is excluded only if the plane elastic solid structural component is considered.

The first variations of the energy bilinear and load linear forms of Eqs. (42–45) are

$$d'_{\delta u}(z_{tt},\bar{z}) = \int\int_\Omega \rho \sum_{i=1}^{3} z_{i,tt}\bar{z}_i \delta h \, d\Omega \tag{46}$$

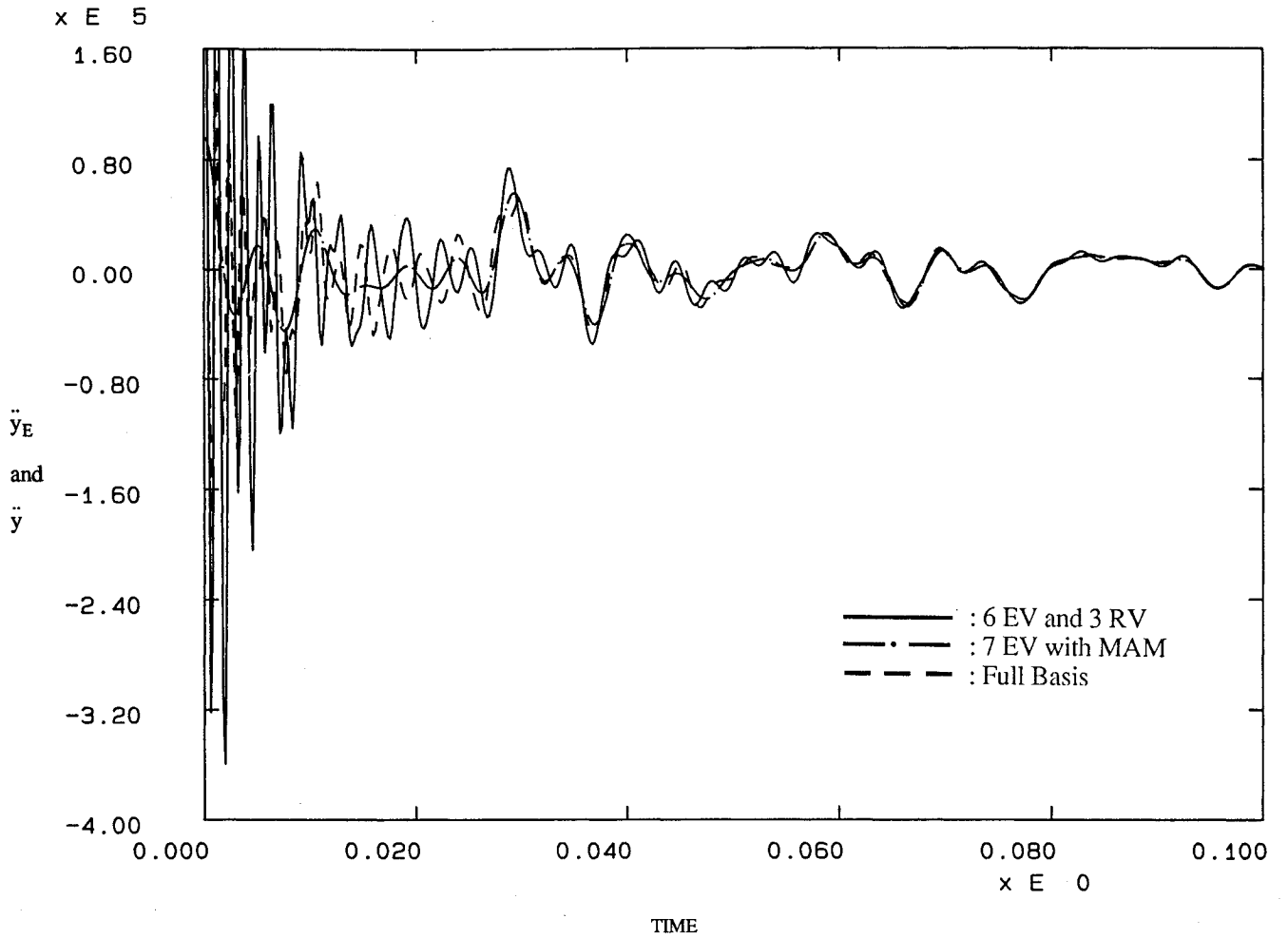

Fig. 8 Comparison of y acceleration at node 27 using the LDRV method and MAM.

$$a'_{\delta u}(z,\bar{z}) = \int\int_{\Omega} \left[\sum_{i,j=1}^{2} \sigma^{ij}(v)\epsilon^{ij}(\bar{v}) + \frac{1}{3} \sum_{i,j=1}^{2} \sigma^{ij}(z_3)\epsilon^{ij}(\bar{z}_3) \right] \delta h \, d\Omega \tag{47}$$

$$\int\int_{\Omega} \bar{z} c_{,u} z_t \, d\Omega = \alpha d'_{\delta u}(z_t,\bar{z}) + \beta a'_{\delta u}(z_t,\bar{z}) \tag{48}$$

$$l'_{\delta u}(\bar{z}) = \int\int_{\Omega} \sum_{i=1}^{3} f_{i,h}\bar{z}_i \delta h \, d\Omega + \int_{\Gamma^2} \sum_{i=1}^{2} T_{i,h}\bar{z}_i \delta h \, d\Gamma \tag{49}$$

where subscript h denotes the derivatives of terms with respect to design variable h.

Consider a performance measure representing a displacement at a discrete point $\hat{x}$ as

$$\Psi_2 = \int_0^T \int\int_{\Omega} \hat{\delta}(x - \hat{x}) z \, d\Omega \, dt \tag{50}$$

The first variation of the performance measure Ψ_2 is

$$\Psi'_2 = \int_0^T \int\int_{\Omega} \hat{\delta}(x - \hat{x}) z' \, d\Omega \, dt \tag{51}$$

VI. Numerical Example

The design sensitivity of pointwise displacements of two undamped structures,[19] a 25-member transmission tower with 18 DOF and a 108-member helicopter tail boom with 72 DOF, are discussed in Refs. 20 and 21, respectively. The helicopter tail boom with Rayleigh damping is studied here using the LDRV method and MAM. The damping coefficients are $0.1318d{+}02$ and $0.2132d{-}04$ for α and β, respectively. This structure is subject to suddenly applied loads. For this structure, design variables are the cross-section areas and performance measures are the displacements of critical points.[22]

ANSYS[23] is used to obtain stiffness and mass matrices, and the eigenvalue problem is solved using EISPACK. A Fortran program is written to generate Ritz vectors, and the Wilson θ method is used for direct integration of the coupled matrix equation in the LDRV method. In the MAM, the Newmark β method is used for direct integration of the uncoupled equation. In this study, an Alliant FX/8[24] is used to obtain the design sensitivity using parallel computation.

LDRV vectors generated using the original load of Eq. (8) might not be a good basis for the fictitious load of the sensitivity equation (18). However, regenerating LDRV vectors at every time step would be very expensive. If the MAM of Eq. (22) is used, the basis vectors do not have to be updated since the fictitious load is taken care of in Eq. (22). The tail boom truss is used to compare these two methods.

The geometry and dimensions of a 108-member helicopter tail boom truss are shown in Fig. 3 and the load data are shown in Fig. 4. The design data and initial design are given in Table 1. The first five natural frequencies, computed by EISPACK, are 34.20, 35.51, 69.93, 98.13, and 101.44 Hz. The time step of 0.0001 s is used for analysis of both original and sensitivity equations. Sizing design sensitivity of pointwise displacements with respect to the first design variable, using the LDRV method and MAM at 0.016 and 0.047 s, which are the first and the second peak times are given in Tables 2–9. In Tables 2–9, the responses in the y direction of the last four nodes only are given because maximum displacements occur at these tip nodes.

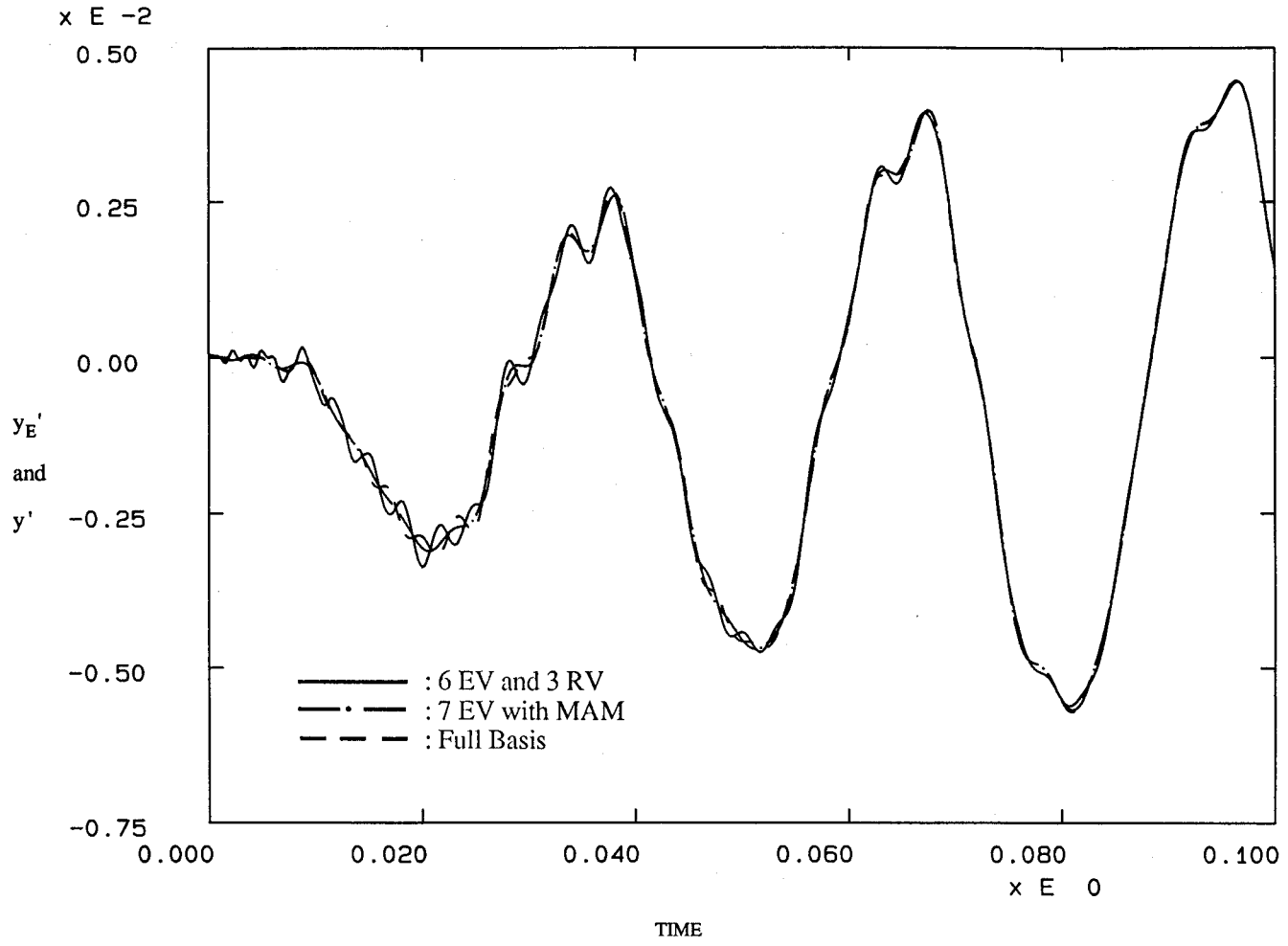

Fig. 9 Comparison of sensitivity prediction using the LDRV method and MAM.

The first design variable is the cross-section areas of members 2 and 3, as shown in Fig. 5.

The central finite difference is denoted by $\Delta\Psi = [\Psi(u + \delta u) - \Psi(u - \delta u)]/2$, and Ψ' is the computed design sensitivity prediction. The ratio between $\Delta\Psi$ and Ψ' times 100 is used as a measure of accuracy of the design sensitivity computation. That is, 100% agreement means that the predicted change is exactly the same as the finite difference result. When $\Delta\Psi$ is too small, this accuracy measure may fail to give correct information because $\Delta\Psi$ may lose numerically significant digits. On the other hand, if $\Delta\Psi$ is too large, the finite difference may contain nonlinear terms. Subscript E denotes the solution that was obtained using full basis vectors with the analytical integration. In these tables, $\Delta\Psi_E/\Psi'$ and $\Delta\Psi_E/\Delta\Psi$ are used to check the accuracy of design sensitivity with the central finite difference of the solution with full basis. Ψ_E/Ψ, $\dot{\Psi}_E/\dot{\Psi}$, and $\ddot{\Psi}_E/\ddot{\Psi}$ represent agreements between displacements, velocities, and accelerations obtained with full and less than full bases, respectively.

Results of the LDRV method using 10 eigenvectors and 5 Ritz vectors are shown in Tables 2 and 3. Tables 4 and 5 contain results of the MAM using 15 eigenvectors. Results of both methods are excellent: the error in $\Delta\Psi_E/\Psi'$ is $<3\%$ for the LDRV method and is $<2\%$ for the MAM. Results of the LDRV method using six eigenvectors and three Ritz vectors are shown in Tables 6 and 7. Tables 8 and 9 contain results of the MAM using seven eigenvectors. These are the minimum numbers of bases that produce $<10\%$ error in $\Delta\Psi_E/\Psi'$ for each method. For the LDRV method, results of these tables indicate that the basis vectors for the original load are good for the fictitious load of the sensitivity equation. However, results of the MAM are slightly better than those of the LDRV method because the displacement using the MAM is updated at every time step using the fictitious load. The time histories of displacement, velocity, acceleration, and sensitivity prediction in the y direction at node 27, where the maximum displacement occurs, are given in Figs. 6–9, respectively. In Figs. 6–9, responses of the LDRV method using six eigenvectors and three Ritz vectors are solid lines, responses of the MAM using seven eigenvectors are dot-dashed lines, and responses of the full basis are dashed lines. In the beginning, responses of both methods using the minimum bases do not agree with responses of the full basis, but become very close after 0.04 s.

VII. Conclusions

A unified continuum-based sizing DSA method for the transient dynamic response of built-up structures, utilizing the direct differentiation and superposition methods, has been proposed. This method is very efficient since derivatives of stiffness and mass matrices are not required. Furthermore, derivatives of basis vectors that demand large computational effort are not required. Last, use of the LDRV method or the MAM makes this method inexpensive and improves the accuracy of analysis results and, thereby, the accuracy of sensitivity. A helicopter tail boom truss with Rayleigh damping using the LDRV method and MAM is studied, and very good design sensitivity results of the pointwise transient response are obtained. The minimum bases that produce $<10\%$ error in the sensitivity prediction are six eigenvectors and three Ritz vectors for the LDRV method and seven eigenvectors for the MAM. For this numerical example, the same number of basis vectors that are used for analysis of the original structure is enough for analysis of the design sensitivity equation.

References

[1]Cornwell, R. E., Craig, R. R., and Johnson, C. P., "On the Application of the Mode Acceleration Method to Structural Engineering Problems," *Earthquake Engineering and Structural Dynamics*, Vol. 11, 1983, pp. 679–688.

[2]Leger, P., and Wilson, E. L., "Modal Summation Methods for Structural Dynamic Computations," *Earthquake Engineering and Structural Dynamics*, Vol. 16, 1988, pp. 23–27.

[3]Wilson, E. L., Yuan, M. W., and Dickens, J. M., "Dynamic Analysis by Direct Superposition of Ritz Vectors," *Earthquake Engineering and Structural Dynamics*, Vol. 10, 1982, pp. 813–821.

[4]Kline, K. A., "Dynamic Analysis Using a Reduced Basis of Exact Modes and Ritz Vectors," *AIAA Journal*, Vol. 24, No. 12, 1986, pp. 2022–2029.

[5]Leger, P., Wilson, E. L., and Clough, R. W., "The Use of Load Dependent Vectors for Dynamic and Earthquake Analysis," Earthquake Engineering Research Center, Univ. of California, Rept. UBC/EERC-86/04, Berkeley, CA, March 1986.

[6]Drucker, D. S., Lou, M., Wang, S., and Kline, K. A., "A Comparison of Mode Acceleration and Ritz Vector Reduced Basis Procedures in Transient Analysis," *Proceedings of 7th International Conference on Vehicle Structural Mechanics*, Detroit, MI, April, 1988, SAE 880908.

[7]Parlett, B. N., *The Symmetric Eigenvalue Problem*, Prentice-Hall, Englewood Cliffs, NJ, 1980.

[8]Nour-Omid, B., and Clough, R. W., "Dynamic Analysis of Structures Using Lanczos Coordinate," *Earthquake Engineering and Structural Dynamics*, Vol. 12, 1984, pp. 565–577.

[9]Kim, H. M., and Craig, R. R., Jr., "Structural Dynamics Analysis Using an Unsymmetric Block Lanczos Algorithm," *International Journal for Numerical Methods in Engineering*, Vol. 26, 1988, pp. 2305–2318.

[10]Haug, E. J., Choi, K. K., and Komkov, V., *Design Sensitivity Analysis of Structural Systems*, Academic, New York, 1986; also, translated to Russian by N. V. Banichuk and published in the USSR, 1988.

[11]Choi, K. K., and Seong, H. G., "A Domain Method for Shape Design Sensitivity Analysis of Built-Up Structures," *Computer Methods in Applied Mechanics and Engineering*, Vol. 57, 1986, pp. 1–15.

[12]Choi, K. K., and Seong, H. G., "Design Component Method for Sensitivity Analysis of Built-Up Structures," *Journal of Structure Mechanics*, Vol. 14, 1986, pp. 379–399.

[13]Choi, K. K., and Santos, J. L. T., "Design Sensitivity Analysis of Nonlinear Structural Systems. Part I: Theory," *International Journal of Numerical Methods in Engineering*, Vol. 24, 1987, pp. 2039–2055.

[14]Santos, J. L. T., and Choi, K. K., "Sizing Design Sensitivty Analysis of Nonlinear Structural Systems. Part II: Numerical Method," *International Journal of Numerical Methods in Engineering*, Vol. 26, 1988, pp. 2097–2114.

[15]Mani, N. K., and Haug, E. J., "Singular Value Decomposition for Dynamic System Design," *Engineering with Computers*, Vol. 1, 1985, pp. 103–109.

[16]Ray, D., Pister, K. S., and Polak, E., "Sensitivity Analysis for Hysteretic Dynamic Systems: Theory and Applications," *Computer Methods in Applied Mechanics and Engineering*, Vol. 14, 1978, pp. 179–208.

[17]Haug, E. J., Wehage, R., and Barman, N. C., "Design Sensitivity Analysis of Planar Mechanism and Machine Dynamics," *Journal of Mechanical Design*, Vol. 103, 1981, pp. 560–570.

[18]Heish, C. C., and Arora, J. S., "Design Sensitivity Analysis and Optimization of Dynamic Response," *Computer Methods in Applied Mechanics and Engineering*, Vol. 43, 1984, pp. 195–219.

[19]Haug, E. J., and Arora, J. S., *Applied Optimal Design*, Wiley, New York, 1979.

[20]Choi, K., and Wang, S., "Continuum Design Sensitivity of Structural Dynamic Response Using Ritz Sequence," *Proceedings of 31st Structures, Structural Dynamics and Materials Conference*, AIAA, Washington, DC, 1990, pp. 385–393.

[21]Choi, K., and Wang, S., "Continuum Design Sensitivity of Structural Dynamic Response Using Ritz Sequence," Center for Simulation and Design Optimization of Mechanical Systems, Univ. of Iowa, Iowa City, IA, TR R-73, May 1990.

[22]Green, W. H., and Haftka, R. T., "Computational Aspects of Sensitivity Calculations in Transient Structural Analysis," *Computers & Structures*, Vol. 32, No. 2, 1989, pp. 433–443.

[23]DeSalvo, G. J., and Swanson, J. A., "ANSYS Engineering Analysis System, *User's Manual*," Vols. I and II, Swanson Analysis Systems, Inc., Houston, PA, 1987.

[24]*FX/Fortran Programmer Handbook*, Alliant Computer Systems Corp., July 1988.